

Water Photovoltaic Pumping System Based on IRFOC Induction Motor Drives

¹Nessrine Chaieb, ²Noureddine Hidouri

¹Faculty of Sciences of Gafsa, Campus Universitaire Sidi Ahmed Zarrouk - 2112 Gafsa, Tunisia

²Preparatory Engineering Institute of Gafsa, Campus Universitaire Sidi Ahmed Zarrouk - 2112 Gafsa, Tunisia

Email: chaieb.nessrine@yahoo.com , noureddine.hidouri@yahoo.fr

Abstract –In this paper, the Authors present an indirect rotor field oriented control of an induction motor (IM) associated to a water photovoltaic pumping system. The motor is used to drive a centrifugal water pump. A modeling study was performed for the components of the proposed photovoltaic pumping system were established and used in the proposed control scheme. An extensive simulation work was performed to extract the significant results. To show up the high system performances, presented results are discussed and prove how the proposed methodology is an efficient water photovoltaic pumping system control procedure.

Keywords – Photovoltaic, water pumping system, induction motor, IRFOC, synchronous boost converter

1. Introduction

In the isolated sectors as the islands, the rural zones and the mountains, the use of the renewable energy such as wind energy [1-3], photovoltaic [4-6] and hybrid system [7-11] is a better solution to produce the needed electric energy for such applications as the pumping systems. The photovoltaic PV water pumping systems are usually composed of a PV generator, power(s) converter(s) and an electric motor which is usually coupled to a centrifugal pump load. Currently, for the power conditioning, the PV generator is followed by a DC-DC converter. Many types are used such as boost, buck and boost-buck converters. Different types of motors are used in the photovoltaic water pumping system. The DC motor is used in the photovoltaic water pumping system with different coupling mode [8], [11], [12]. The Permanent Magnet Synchronous Motors (PMSM) is also used with different control strategies [4], [13]. Some applications of the pumping system call for the asynchronous motor [9], [10]. Many techniques of control have been applied to induction motor as direct

torque control (DTC) and field oriented control. The concept of field oriented control (FOC) is firstly developed by Blasche,[14]. The FOC is a flux-torque decoupling technique applied to AC machines. Two approaches are possible: the direct field orientation (DFO) based on the rotor flux angle given by a flux observer or estimator and the indirect field orientation (IFO) based on the rotor slip calculation, [15], [16].

In this paper an indirect rotor field oriented control is synthesized for an induction motor (IM) associated to a water photovoltaic pumping system in order to produce the required load power. A synchronous boost converter is used in the control scheme to adapt the DC voltage required by the load when the insulation or the load varies.

2. The IM Photovoltaic pumping system model

The proposed IM photovoltaic pumping system considered in this work is shown in figure 1.

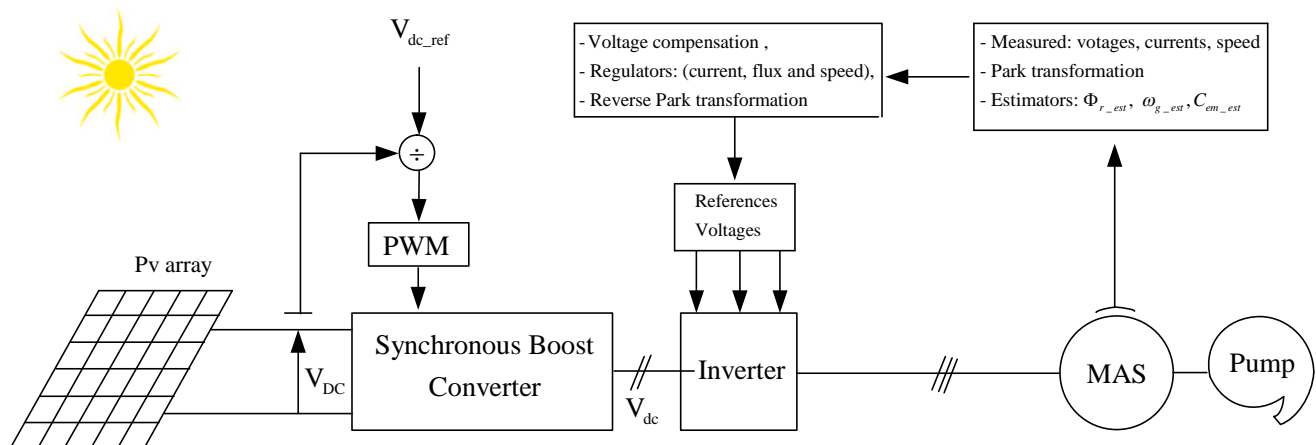


Figure 1. The proposed IM photovoltaic pumping system configuration

In order to convert the mechanical power to electrical power required by the load, the stator of the induction motor is supplied by a three phase inverter. The V_{dc} voltage required by the inverter is provided by the PV panel through the PWM controlled synchronous boost converter.

2.1. Cell and PV Models

The solar cell is an electric component that is used for technologically converting the solar energy into electricity to produce the electrical energy needs in some application requirement. In order to prove their research work, many authors proposed different models for the solar cell [4], [17-20]. The electric model of a solar cell is shown in figure 2 where I_{ph} , D , R_{sc} and R_{pc} represent respectively the light-generated current source, the diode, the series and parallel resistances.

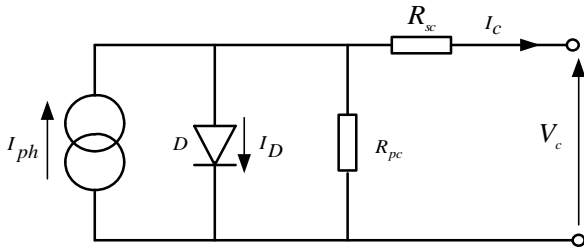


Figure 2. Equivalent solar cell's electric circuit

At the reference condition defined by the cell junction temperature T_{c_ref} and the insulation G_{ref} , the photocurrent I_{ph_ref} is equal to the reverse saturation current I_{sc_ref} .

At the desired cell junction temperature T_c and the insulation G , the cell photocurrent I_{ph} can be deduced from the reference data condition given by equation where K_{SCT} stands for the short circuit current temperature coefficient.

$$I_{ph} = \frac{G}{G_{ref}} \left(I_{sc_ref} + K_{SCT} (T_c - T_{c_ref}) \right) \quad (1)$$

The desired reverse saturation current I_{rs} is also obtained from the reference condition according to relation (2), where E_g , q , k and β represent respectively the band gap energy of the semiconductor, the electron charge, the ideal factor off the solar cell and the Boltzmann constant.

$$I_{rs} = I_{rs_ref} \left(\frac{T_c}{T_{c_ref}} \right)^3 \exp \left[\frac{qE_g}{\beta k} \left(\frac{1}{T_c} - \frac{1}{T_{c_ref}} \right) \right] \quad (2)$$

Many others express the characteristic equation relating the cell's current I_c to its voltage V_c as represented in (3).

$$I_c = I_{ph} - I_{rs} \left(\exp \left(\frac{q}{\beta k T_c} (V_c + R_{sc} I_c) \right) - 1 \right) - \frac{(V_c + R_{sc} I_c)}{R_{pc}} \quad (3)$$

The solar panel can be composed of N_p array of modules assembled in parallel; each one can be composed of N_s modules assembled in series. A module can also contain n_s cells associated in series configuration. This consideration expresses the relations between the panel's and the cells parameters, relation (4).

$$\begin{cases} I_p = N_p I_c \\ V_p = n_s N_s V_c \\ R_{sp} = \frac{n_s N_s}{N_p} R_{sc} \\ R_{pp} = \frac{n_s N_s}{N_p} R_{pc} \end{cases} \quad (4)$$

In this consideration, the non-linear characteristic equation related the panel current I_p to its voltage V_p is shown in (5).

$$I_p = N_p I_{ph} - N_p I_{rs} \left(\exp \frac{q}{\beta k T_c} \left(\frac{V_p}{n_s N_s} + \frac{R_{sc} I_p}{N_p} \right) - 1 \right) - \frac{N_p}{R_{pc}} \left(\frac{V_p}{n_s N_s} + \frac{R_{sc} I_p}{N_p} \right) \quad (5)$$

2.2 Asynchronous Motor Model

In the Concordia reference frame, the direct and the quadratic components of the stator voltage are given by relation (6).

$$\begin{cases} v_{sd} = R_s i_{sd} + \frac{d\varphi_{sd}}{dt} \\ v_{sq} = R_s i_{sq} + \frac{d\varphi_{sq}}{dt} \end{cases} \quad (6)$$

The direct and the quadratic components of the stator flux and the rotor flux are respectively given by relations (7) and (8).

$$\begin{cases} \varphi_{sd} = L_s i_{sd} + M_{sr} i_{rd} \\ \varphi_{sq} = M_{rs} i_{rq} + L_s i_{sq} \end{cases} \quad (7)$$

$$\begin{cases} \varphi_{rd} = L_r i_{rd} + M_{sr} i_{sd} \\ \varphi_{rq} = M_{rs} i_{sq} + L_r i_{rq} \end{cases} \quad (8)$$

The electromagnetic torque can be expressed by relation (9) where p represents the motor pair pole number.

$$C_{em} = p \frac{M_{sr}}{L_r} (\varphi_{rd} i_{sq} - \varphi_{rq} i_{sd}) \quad (9)$$

When Park synchronous reference frame with the stator flux is used, (6) becomes as follows, where ω_s is the electric stator flux speed:

$$\begin{cases} V_{sd} = R_s I_{sd} + \frac{d\Phi_{sd}}{dt} - \omega_s \Phi_{sq} \\ V_{sq} = R_s I_{sq} + \frac{d\Phi_{sq}}{dt} + \omega_s \Phi_{sd} \end{cases} \quad (10)$$

The components of stator flux and rotor flux vectors are linked to those of current vector by:

$$\begin{cases} \Phi_{sd} = L_s I_{sd} + M_{sr} I_{rd} \\ \Phi_{sq} = M_{rs} I_{rq} + L_s I_{sq} \end{cases} \quad (11)$$

$$\begin{cases} \Phi_{rd} = L_r I_{rd} + M_{sr} I_{sd} \\ \Phi_{rq} = M_{rs} I_{sq} + L_r I_{rq} \end{cases} \quad (12)$$

The electromagnetic torque can be expressed by relation (13)

$$C_{em} = p \frac{M_{sr}}{L_r} (\Phi_{rd} I_{sq} - \Phi_{rq} I_{sd}) \quad (13)$$

2.3. Centrifugal pump model

The centrifugal pump model can be described by the well known mechanical characteristic illustrated in relation (14).

$$h = a_0 \omega_r^2 - a_1 \omega_r Q - a_2 Q^2 \quad (14)$$

The hydraulic power P_H and the load torque of the centrifugal pump can be described respectively by (15) and (16).

$$P_H = \rho g H \quad (15)$$

$$C_r = k_r \Omega^2 + C_s \quad (16)$$

The mechanical model of the electric motor can be described by (17) where f_m and C_r represent respectively the motor's friction coefficient and the hydraulic load torque of the centrifugal pump.

$$C_{em} = J_m \frac{d\Omega_m}{dt} + f_m \Omega_m + C_r \quad (17)$$

2.4. Synchronous Boost Converter Model

Figure 3 shows the structure of the famous synchronous boost converter used in this research work, [8]. As an assumption, the power devices are considered to be ideal. This idea leads to the consideration that when

the one considered IGBT is open, the current equals zero, and when it is closed, the voltage is zero as well. Also, both capacitive and inductive losses are neglected.

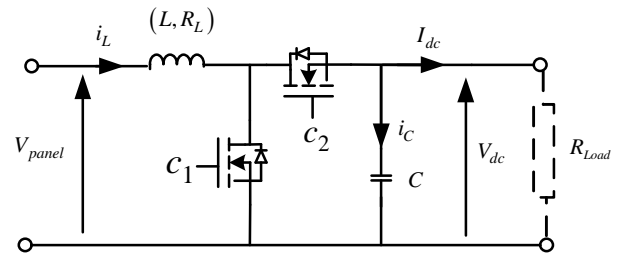


Figure 3. Structure of the boost converter

Relatively to the synchronous boost-converter command, the IGBT state is defined by the PWM signal that is characterized by the duty cycle α and the operating period T .

During the considered operating time period T , the IGBT1 is switched on in αT and switched off in $(1-\alpha)T$ intervals. Inversely the IGBT2 is switched off in αT and switched on in $(1-\alpha)T$ intervals.

As a first consideration, one can focus on the αT interval where the IGBT1 is switched on; however, the IGBT2 is normally switched off.

The state space representation of the synchronous boost converter with respect to the αT interval can be deduced as :

$$\begin{bmatrix} \dot{i}_L \\ \dot{V}_C \end{bmatrix} = \begin{bmatrix} -\frac{R_L}{L} & 0 \\ 0 & -\frac{1}{R_{Load}C} \end{bmatrix} \begin{bmatrix} i_L \\ V_C \end{bmatrix} + \begin{bmatrix} \frac{1}{L} \\ 0 \end{bmatrix} V_{panel} \quad (18)$$

$$V_{dc} = [0 \ 1] [i_L \ V_C]^t \quad (19)$$

Considering the $(1-\alpha)T$ interval, the IGBT1 is switched off and the IGBT2 is switched on.

The state space representation of the synchronous boost converter for this interval can be deduced as:

$$\begin{bmatrix} \dot{i}_L \\ \dot{V}_C \end{bmatrix} = \begin{bmatrix} -\frac{R_L}{L} & -\frac{1}{L} \\ \frac{1}{C} & -\frac{1}{R_{Load}C} \end{bmatrix} \begin{bmatrix} i_L \\ V_C \end{bmatrix} + \begin{bmatrix} \frac{1}{L} \\ 0 \end{bmatrix} V_{panel} \quad (20)$$

$$V_{dc} = [0 \ 1] [i_L \ V_C]^t \quad (21)$$

During the two intervals presented previously, the converter model can be obtained by merging the two state models (eq. (18) and(20)) presented above relatively to the two intervals with respect to the IGBT state.

The average's boost converts model is given by (22) and (23) where the control term α designate the duty cycle indicating the converter action in the global model:

$$\begin{bmatrix} \bullet \\ i_L \\ \bullet \\ V_C \end{bmatrix} = \begin{bmatrix} -\frac{R_L}{L} & -\frac{1-\alpha}{L} \\ \frac{1-\alpha}{C} & -\frac{1}{R_{Load}C} \end{bmatrix} \begin{bmatrix} i_L \\ V_C \end{bmatrix} + \begin{bmatrix} \frac{1}{L} \\ 0 \end{bmatrix} V_{panel} \quad (22)$$

$$V_{dc} = [0 \ 1][i_L \ V_C]^T \quad (23)$$

If we designate by $(c_1 = 1 - c_2)$ a Boolean variable that takes the value $(c_1 = 0)$ if the IGBT1 is switched off and the IGBT2 is switched on and takes the value $(c_1 = 1)$ if the IGBT1 is switched on and the IGBT2 is switched off. According to this idea, the new global model taking account of the boost converter model is given as:

$$\begin{bmatrix} \bullet \\ i_L \\ \bullet \\ V_C \end{bmatrix} = \begin{bmatrix} -\frac{R_L}{L} & -\frac{1-c_1}{L} \\ \frac{1-c_1}{C} & -\frac{1}{R_{Load}C} \end{bmatrix} \begin{bmatrix} i_L \\ V_C \end{bmatrix} + \begin{bmatrix} \frac{1}{L} \\ 0 \end{bmatrix} V_{panel} \quad (24)$$

$$V_{dc} = [0 \ 1][i_L \ V_C]^T \quad (25)$$

3. The IM field-oriented control strategy

After arrangement, the system of equation (10) can be represented by (26) where the different related terms are given by (27) and (28).

$$\begin{cases} V_{sd} = V_{sd1} - E_d \\ V_{sq} = V_{sq1} - E_q \end{cases} \quad (26)$$

$$\begin{cases} V_{sd1} = \sigma L_s \frac{dI_{sd}}{dt} + \left(R_s + R_r \frac{M_{sr}^2}{L_r^2} \right) I_{sd} \\ V_{sq1} = \sigma L_s \frac{dI_{sq}}{dt} + \left(R_s + R_r \frac{M_{sr}^2}{L_r^2} \right) I_{sq} \end{cases} \quad (27)$$

$$\begin{cases} E_d = \frac{M_{sr}R_r}{L_r^2} \Phi_{rd} + \frac{M_{sr}\omega_r}{L_r} \Phi_{rq} + \sigma L_s \omega_s I_{sq} \\ E_q = -\sigma L_s \omega_s I_{sd} - \frac{M_{sr}\omega_r}{L_r} \Phi_{rd} + \frac{M_{sr}R_r}{L_r^2} \Phi_{rq} \end{cases} \quad (28)$$

Considering the rotor flux orientation condition given by relation (29) and the famous relation (30), equation (28) can be simplified to (31).

$$\begin{cases} \Phi_{rd} = \Phi_r \\ \Phi_{rq} = 0 \end{cases} \quad (29)$$

$$\omega_s = \omega_r + \frac{M_{sr}R_r}{L_r\Phi_r} I_{sq} \quad (30)$$

$$\begin{cases} E_d = \frac{M_{sr}R_r}{L_r^2} \Phi_r + \sigma L_s \omega_s I_{sq} \\ E_q = -\sigma L_s \omega_s I_{sd} - \frac{M_{sr}\omega_s}{L_r} \Phi_r + \frac{M_{sr}^2 R_r}{L_r^2} I_{sq} \end{cases} \quad (31)$$

3.2 Estimation of the rotor flux, the slip frequency and the electromagnetic torque

The rotor flux can be estimated from the quadratic stator current component obtained when the park transformation is applied to the measured three stator currents as indicated by the will known relation (32).

$$\Phi_{r_est} = \frac{M_{sr}}{1 + \frac{L_r}{R_r} p} I_{sd} \quad (32)$$

The slip frequency (33) is estimated from the quadratic current and the estimated rotor flux.

$$\omega_{g_est} = \frac{M_{sr}}{R_r} \frac{I_{sq}}{\Phi_{r_est}} \quad (33)$$

The expression of the estimated electromagnetic torque is given by relation (34).

$$C_{em_est} = p \frac{M_{sr}}{L_r} \Phi_{r_est} I_{sq} \quad (34)$$

3.2 Regulation of the stator current

The direct and the quadratic transfer functions current/voltage are respectively given by (35) and (36).

$$H_{Id}(p) = \frac{I_{sd}}{V_{sd1}} = \frac{\frac{1}{R_s + R_r \frac{M_{sr}^2}{L_r^2}}}{1 + \frac{\sigma L_s}{R_s + R_r \frac{M_{sr}^2}{L_r^2}} p} \quad (35)$$

$$H_{Iq}(p) = \frac{I_{sq}}{V_{sq1}} = \frac{\frac{1}{R_s + R_r \frac{M_{sr}^2}{L_r^2}}}{1 + \frac{\sigma L_s}{R_s + R_r \frac{M_{sr}^2}{L_r^2}} p} \quad (36)$$

If the pole-zero cancellation method is used, the expressions and the parameters of the PI current controller can be respectively expressed by (37) and (38).

$$\begin{cases} C_{ld}(p) = K_{ld} \left(1 + \frac{1}{\tau_{ld} p} \right) \\ C_{lq}(p) = K_{lq} \left(1 + \frac{1}{\tau_{lq} p} \right) \end{cases} \quad (37)$$

$$\begin{cases} K_{ld} = K_{lq} = \left(R_s + R_r \frac{M_{sr}^2}{L_r^2} \right) \\ \tau_{ld} = \tau_{lq} = \frac{\sigma L_s}{R_s + R_r \frac{M_{sr}^2}{L_r^2}} \end{cases} \quad (38)$$

3.3 Regulation of the rotor flux

The transfer function flux/current is given by:

$$H_{\Phi rd}(p) = \frac{\Phi_{rd}}{I_{sd}} = \frac{M_{sr}}{1 + \frac{L_r}{R_r} p} \quad (39)$$

If the pole-zero cancellation method is used, the expressions and the parameters of the PI flux controller can be expressed by (40).

$$\begin{cases} C_{\Phi}(p) = K_{\Phi} \left(1 + \frac{1}{\tau_{\Phi} p} \right) \\ K_{\Phi} = \frac{1}{M_{sr}}; \tau_{\Phi} = \frac{L_r}{R_r} \end{cases} \quad (40)$$

3.4 Regulation of the rotor speed

As shown by figure 4, a PI regulator is used to control the speed.

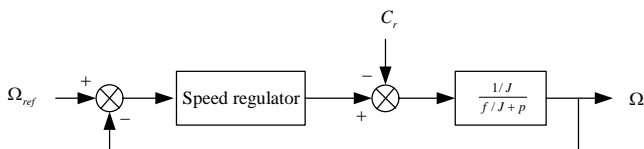


Figure 4. Bloc diagram of the speed regulator

$$\Omega = \frac{(k_{p\omega} \cdot p + k_{i\omega}) \Omega_{ref} - p C_r}{J \cdot p^2 + (k_{p\omega} + f) \cdot p + k_{i\omega}} \quad (41)$$

The denominator of relation (41) shows that the system has a dynamic of second order that can be identified with the canonical form $1 + \frac{2\xi}{\omega_n} p + \frac{p^2}{\omega_n^2}$. In this consideration, the parameters of the PI speed controller are expressed by (42).

$$\begin{cases} \frac{J}{K_{i\omega}} = \frac{1}{\omega_n^2} \\ \frac{2\xi}{\omega_n} = \frac{K_{p\omega} + f}{K_{i\omega}} \end{cases} \quad (42)$$

4. Simulation results and discussion

The simulation in this work has been developed in Matlab/Simulink environment.

In this study, we consider that the load is fed by the PV array through a boost converter.

4.1 Analyzes of physical sizes relating to the photovoltaic panel and the boost converter

The command of the boost converter is based on the DC voltage required by the load. This value is computed as a reference boost voltage term. The figures 5 and 6 give respectively the panel's and the output boost converter voltages. The second one (figure 6) converges towards the required DC voltage according to the first one.

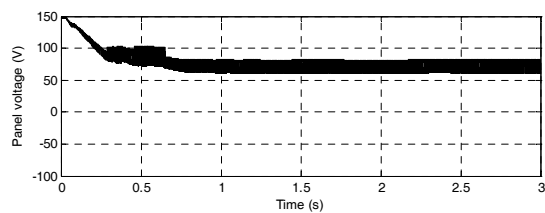


Figure 5. The panel voltage

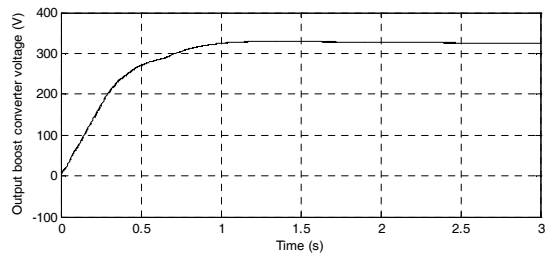


Figure 6. Output boost converter voltage

Figure 7 shows that panel current is perfectly continuous with a good choice of the capacitance value relatively to that of the inductance.

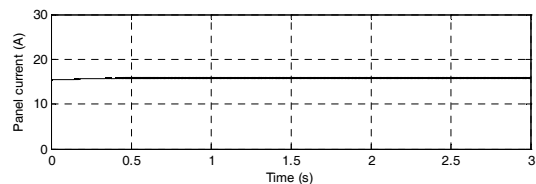


Figure 7. The panel current

4.2. Analyzes of physical sizes relating to the induction motor

Initially, the induction motor is at stopped, at $t = 0$, a reference direct rotor flux and a reference electric speed was applied to the motor.

The reference and estimated direct rotor fluxes are respectively given by figure 8 and figure 9. It's shown that the estimated converges strictly to the reference one.

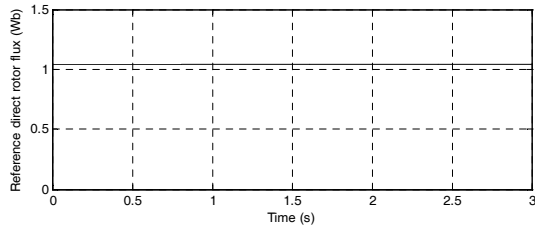


Figure 8. Reference direct rotor flux

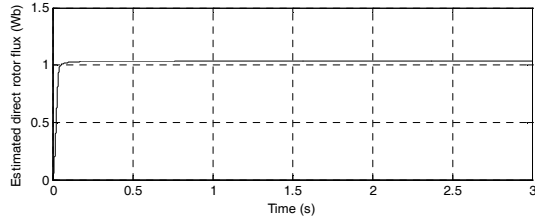


Figure 9. Estimated direct rotor flux

Related to figure 9 (estimated direct rotor flux), figure 10 shows that the quadratic component rotor flux converges to zero as an improvement that the rotor flux is oriented to the direct axis.

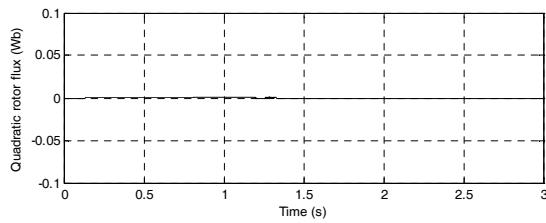


Figure 10. Quadratic rotor flux

Figure 11 and figure 12 show that, the electric rotor speed converges to the reference one.

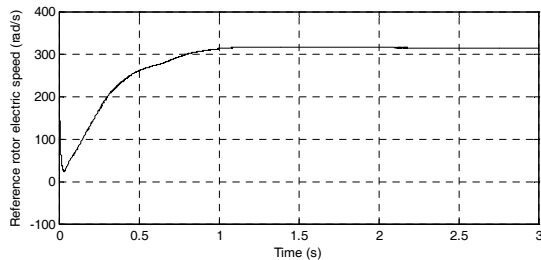


Figure 11. Reference electric rotor speed

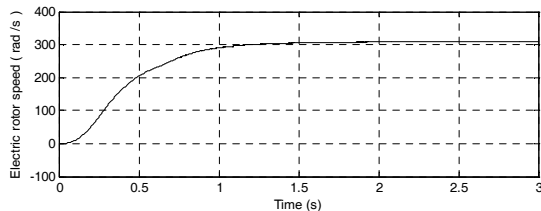


Figure 12. Response of the electric rotor speed

The electromagnetic torque response (figure 13) as well as the estimated electromagnetic torque (figure 14) converge towards their target ones (rated values).

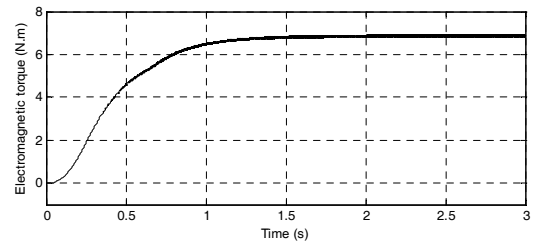


Figure 13. Electromagnetic torque

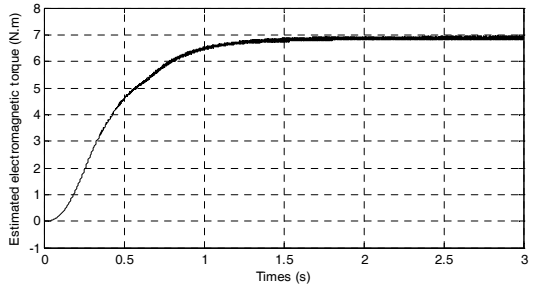


Figure 14. Estimated electromagnetic torque

Appendix

Table 1. Induction motor Parameters

Rated voltage V_{sN}	240 V
Rated current I_N	4.2 A
Rated speed Ω_N	157 rad / s
Pole pairs p	2
Rotor resistance R_r	4.3 Ω
Stator resistance R_s	9.65 Ω
Stator inductance L_s	471.8 mH
Rotor inductance L_r	471.8 mH
Magnetizing inductance M_{sr}	447.5 mH

Table 2. Parameters of Pv module

Rated output power	216W
Open circuit voltage: V_{oc}	36.35 V
Number of series cells: n_s	60

Table 3. Parameters of Pv Cell (Polly-crystalline silicon)

Open circuit voltage: V_{oc}	0.6058 V
Short circuit current : I_{sc}	8.1 A
Parallel cell's resistance: R_{pc}	0.833 Ω
Series cell's resistance: R_{sc}	0.0833 m Ω
Solar cell's ideal factor : k	1.450
reverse diode saturation current I_{rs}	3.047e-7 A
Short circuit current temperature coefficient K_{SCT}	1.73e-3 A/ $^{\circ}$ K
Reference cell's temperature: T_{c_ref}	25 $^{\circ}$ C
Boltzmann's constant: β	1.38e-23
Band gap energy: E_g	1.11 eV

Table 4. PV Array Parameters

Open circuit voltage: V_{oc}	254 V
Short circuit current : I_{sc}	8.1 A
Number of series modules: N_s	7
Number of parallel modules: N_p	2

. References

- [1] N. Hidouri, S. Hammadi, L. Sbita, An Isolated Boost PMSG-Wind-Turbine System Based on Direct Torque Control Drive Scheme, *International Journal of Research and Reviews in Science (IJRRCS)*, vol. 2, No. 3, (2011), pp. 753-760.
- [2] H. Jedli, N. Hidouri, A Power Drive Scheme for an Isolated Pitched Wind Turbine Water Pumping System based on DC machine, *Advance in Mechanical Engineering and Application*, Vol. 1.1,(2012), pp. 1-4.
- [3] Tomás Perpétuo Corrêa, Seleme Isaac Seleme Jr., Selênio Rocha Silva, "Efficiency optimization in stand-alone photovoltaic pumping system", *Renewable Energy*, Volume 41, (2012), pp 220-226.
- [4] N. Hidouri, L. Sbita, A New DTC-SPMSM Drive Scheme for PV Pumping System, *International Journal of Systems Control*, vol.1.3, (2010), pp. 113-121.
- [5] M. Makhoulouf, F. Messai, H. Benalla, vectored command of induction motor pumping system supplied by photovoltaic generator, *Journal of ELECTRICAL ENGINEERING*, VOL. 62, NO. 1, 2011 pp. 3–10.
- [6] J. C. Mayo-Maldonado, R. Salas-Cabrera, H. Cisneros-Villegas, R. Castillo-Ibarra, J. Roman-Flores, M. A. Hernandez-Colin, Maximum Power Point Tracking Control for a DC-Generator/Multiplier-Converter Combination for Wind Energy Applications, *Proceedings of the World Congress on Engineering and Computer Science*, Vol I WCECS, San Francisco, USA, October 19-21, (2011).
- [7] N. Hidouri, T. Mhamdi, S. Hammadi, L. Sbita, A New hybrid photovoltaic-diesel system control scheme for an isolated load, *International Journal of Research and Reviews in Applied Sciences*, vol. 9.2, (2011), pp. 270-281.
- [8] A. Hammouda, N. Hidouri, A Voltage Drive Scheme for an Isolated Hybrid Diesel-Photovoltaic Water Pumping System based on DC machine, *Advances in Electrical Engineering Systems* Vol. 1, No. 2, (2012), pp. 82-88.
- [9] Deokar, S.A., Waghmare, L.M., Jadhav, G.N., Voltage flicker assessment of induction motors used in the integrated water pumping station, *International Conference on Power Electronics, Drives and Energy Systems & 2010 Power India*
- [10] M. Makhoulouf, F. Messai, H. Benalla, vectored command of induction motor pumping system supplied by photovoltaic generator, *Journal of ELECTRICAL ENGINEERING*, VOL. 62, NO. 1, 2011 pp. 3–10.
- [11] A. M. Kassem, Modeling, Analysis and Neural MPPT Control Design of a PV Generator Powered DC Motor-Pump System, *WSEAS TRANSACTIONS on SYSTEMS*, Issue 12, Volume 10.12, (2011), pp. 399-412
- [12] A. Terki, A. Moussi, A. Betka, N. Terki, An improved efficiency of fuzzy logic control of PMLBDC for PV pumping system, *Applied Mathematical Modelling*, Volume 36, No 3, (2012), pp. 934 – 944
- [13] Klaus Raggl, Bernhard Warberger, Thomas Nussbaumer, Simon Burger, and Johann W. Kolar, Robust Angle-Sensorless Control of a PMSM Bearingless Pump, *IEEE Transactions on industrial electronics*, Vol. 56, No. 6, JUNE (2009), pp. 2076-2085.
- [14] BLASCHKE. F, The principle of field orientation as applied to the new transvector closed-loop control system for rotating-field machines, *Siemens Review*, vol. 39, No 5, (1972), pp. 217-220.
- [15] S. peresada, A. Tonielli, R. Morici. High - performance indirect field-oriented output-feedback control of induction motors, *Automatica*, Vol 35, (1999), pp. 1033-1047.
- [16] H. Rehman, A. Dhouadi. A Fuzzy learning-sliding mode controller for direct field-oriented induction machines. *Neurocomputing* Vol.71, (2008), pp. 2693-2701.
- [17] T. Bjazic, Z. Ban, I. Volaric, Control of a Fuel Cell Stack loaded with DC/DC Boost Converter, *Industrial Electronics. IEEE International Symposium*, (2008), pp. 1489–1494.
- [18] R. Chenni, M. Makhoulouf, T. Kerbache, A. Bouzid, A detailed modeling method for photovoltaic cells, *Energy*, vol 32, (2008), pp. 1724–1730.
- [19] K.H. Chao, S.H. Ho, M.H. Wang, Modeling and fault diagnosis of a photovoltaic system, *Electric Power Systems Research*, vol.78, (2008), pp.97–105.
- [20] L.S.Kim, Sliding mode controller for the single phase grid-connected photovoltaic system, *Applied Energy*, vol.83, (2006), pp. 1101–1115.